Coordination of A Three Level STATCOM and Enhanced Field Oriented Controller for Grid Connected DFIG to Improve Performance during Different Faults

D V N Ananth and G V Nagesh Kumar

[1]Dept. of Electrical & Electronics Engineering, DADI Institute of Engineering and Tech., Anakapalli, India,
Tel:+91-8500265310, Email: nagaananth@gmail.com
[2]Dept. of Electrical & Electronics Engineering, VIGNAN's Institute of Information Technology, Visakhapatnam, India,
Tel: +91-9000573759, Email: drgvnk14@gmail.com

Abstract: *With the increase in electric power demand, raise at oil prices, transmission lines were forced to operate near to its full load and due to the drastic change in weather conditions, the thermal limit is increasing and the system is operating with less security margin. To meet increased power demand, DFIG based wind generation system is a better alternative. For improving power flow capability and to increase security STATCOM can be adopted. As per modern grid rules, DFIG needs to operate without losing synchronism called Low Voltage Ride Through (LVRT) during severe grid faults. Hence for this, enhanced field oriented control technique (EFOC) was adopted in Rotor Side Control (RSC) of DFIG converter to improve power flow transfer and to improve dynamic and transient stability. The paper has an objective to damp pulsations in electromagnetic oscillations, improve voltage mitigation and limit surge currents and to enhance the operation of DFIG during symmetrical and asymmetrical faults. A three level STATCOM is coordinated to the system for obtaining much better stability and enhanced operation during the grid fault. The STATCOM DC capacitor bank and DFIG converters are connected to a common DC point has advantages like improved real and reactive power flow control in STATCOM, better reactive power support from RSC and GSC with nearly constant DC link voltage maintenance and faster dynamic and transient operation during severe grid faults. For EFOC technique, rotor flux reference changes its value from synchronous speed to zero during fault for injecting current at the rotor slip frequency. In this process DC-Offset component of flux is controlled, decomposition during symmetric and asymmetric faults. The offset decomposition of flux will be oscillatory in a conventional FOC, whereas in EFOC it was aimed to damp quickly. The system performance with different phases to ground faults like SLG, DLG and TLG were applied and compared without and with a three level STATCOM, with fault occurring at the point of common coupling with the fault resistance of very small value at 0.001 ohms.*

Key words: DFIG, Field Oriented Control (FOC), Low Voltage Fault Ride through (LVRT), STATCOM, symmetrical faults, voltage mitigation.

1. INTRODUCTION

The doubly fed induction generator (DFIG) is having a better preference due to its low power ratings of converters, small size with higher MVA ratings available in the market, variable generator speed and constant frequency operation, robust four quadrant reactive power control and much better performance during the low voltage ride through (LVRT). However, such DFIG is sensitive to external disturbances like the voltage sag. If grid voltage falls suddenly due to any reason, large surge currents enter rotor terminals and voltage induces drastically. Hence, the rotor side converter (RSC) will get damaged due to exceeding voltage or the current rating. Apart from this, there will be huge electromagnetic torque pulsations and increase in rotor speed which may reduce gears of the wind turbine-generator lifetime.

The status of research on the LVRT issue for DFIG for symmetrical and asymmetrical faults and comparison of different control strategies is given in [1]. Understanding the capability of RSC to deliver desired reactive power and withstanding capability during the fault in [2]. LVRT enhancement based on flux trajectory [3], enhanced reactive power support [4], controlling DC link current of RSC to smoothen DC voltage fluctuations due to grid faults by using stored Kinetic Energy [5], crowbar as passive and RSC strategy as active compensation for LVRT Q compensation [6], FFTC scheme with PIR [7] and PI [8] with symmetrical and asymmetrical faults for improving uninterrupted P, Q supply from WT to grid. Few intelligent control techniques like Genetic Algorithm [9] and bacterial search etc were used in control strategies for improving the performance during LVRT.

Some external passive elements and active sources are used in coordination for improving stability and thereby providing a better LVRT operation of DFIG during symmetrical and asymmetrical faults. Among external devices which were connected in coordination with DFIG system to enhance system LVRT behavior during severe faults is Single phase crowbar [11], Supercapacitor energy storage system [12], Fault Current Limiter (FCL) [13], Superconducting FCL with Magnetic Energy storage devices [14] were used recently.

Among FACTS family, STATCOM [15-22] is used to overcome the system to lose synchronism because of external disturbances like large variations in wind speed, symmetrical and asymmetrical faults and sub-synchronous resonance. For external grid fault disturbances, hybrid PI (PI +FUZZY) controller is used to improve stability during severe faults [15]. Improvement of voltage stability, damping of electric power system oscillations were achieved in [16, 17]. Heuristic programming and radial basis neural network is used to compensate the voltage sag [18]. In [19 and 20], offshore multiple wind turbine based

DFIG system was connected to a common bus and transferred by using HVDC network. In these papers, STATCOM sizing was decreased by optimal designing of the capacitor for VSC was done. Subsynchronous resonance (SSR) type disturbance was compensated using TCSC, SVC, and STATCOM using root-locus method [21]. Two sequence components with dual voltage control during grid faults for DFIG-STATCOM system were done in [22 and 23]. The DVR with high-temperature SCFCL is used to find the solution for balanced and unbalanced faults at the grid for DFIG system [24]. Frequency domain approach with Eigen analysis was applied for seashore wind farm having DFIG and SCIG to improve power system stability was done in [25] by applying an UPFC controller. Using superconducting coil as energy storage device as integrated into DC link for DFIG system is in [26].

The system performance during a single line to the ground (SLG), double line to ground DLG and triple line to ground (TLG) is compared with and without STATCOM. The voltage and current parameters at the rotor, stator, grid, stator terminal and STATCOM and DFIG electromagnetic torque, the speed of the rotor, DC voltage across back to back converters of DFIG were compared and analyzed under different faults. The three level STATCOM DC link capacitor terminals are connected to the common point at back-to-back of DFIG converters to improve voltage profile at DC coupling point. By doing so, STATCOM can share reactive power as well as active power for compensation at different load angles. This additional reactive source (STATCOM) having higher capacitance value helps in improving DC voltage profile in coordination to GSC and an additional reactive power source for RSC converter. The proposed EFOC method can be applicable to both asymmetrical and symmetrical faults, which help in improving current and voltage profile at stator and rotor terminals during the fault. Much better performance DFIG operation can be expected if an additional reactive power source likes STATCOM is incorporated into the system. The rating of this additional reactive power source can be small but need to be faster at the start and end of the fault. Hence for this STATCOM controller for three levels is designed to improve dynamic stability during asymmetrical or symmetrical faults.

In the section number 2, mathematical modeling of proposed EFOC for rotor side converter (RSC) to the grid connected DFIG is explained during the steady state in section 2a and behavior of DFIG during a symmetrical fault in section 2b. In section 3, the design of coordinated STATCOM for the LVRT issue is described. Further sections 4 describe the simulation results and section 5 describe a detailed discussion on the results in comparison without and with STATCOM in MATLAB environment. The conclusion is given in section 6 followed by appendix and references.

2. Mathematical analysis of RSC and GSC converters for the grid connected DFIG during steady state

The conventional field oriented control (FOC) scheme for DFIG is done in a synchronously rotating frame to facilitate for decoupled active and reactive power control and to enhance the system performance due to transients by improving the dynamic response. The DFIG equivalent circuit [1], [2], [10] and [29], the dynamics of vectors are shown in GSC and RSC control strategies in Fig. 1 and 2. The outer control loop for GSC control scheme for extracting relation with wind speed and mechanical power is done as per the table 1.

Table 1: Lookup table showing the relation of wind speed, rotor speed, mechanical power and output torque for certain speeds.

$V_{wind}\ (m/s)$	7	8	9	10	11	12	18
w_r (pu)	0.75	0.85	0.95	1.05	1.1	1.2	1.3
P_m (pu)	0.32	0.49	0.69	0.9	1	1.15	1.5
$T_{m=\frac{P_m}{w_r}}$ (pu)	0.48	0.58	0.73	0.85	0.9	0.95	1.15

2A. Rotor Side Converter Control

RSC controller helps in improving reactive power demand at g_{rid} in extracting maximum power from the machine for which the rotor is made to run at optimal speed. The optimal speed of the rotor is decided from machine real power and rotor speed characteristic curves from MPPT algorithm. The stator active and reactive power control is possible with the RSC controller strategy through i_{qr} and i_{dr} components controlling respectively. The rotor voltage in a stationary reference frame [11 and 29] is given by

$$V_r^s = V_{0r}^s + R_r i_r^s + \sigma L_r \frac{di_r^s}{dt} - j\omega i_r^s \quad (1a)$$

where, $\sigma = 1 - \frac{L_{sm}^2}{L_s L_r}$ and ω is the rotor speed, i_r^s is the rotor current in a stationary frame of reference, Ls, L_r and Lm are stator, the rotor and mutual inductance parameters in Henry or in pu

$$V_{0r}^s = \frac{L_m}{L_s}\left(\frac{d}{dt} - j\omega_s\right)\Phi_s^s \quad (1b)$$

It is the voltage induced in the stator flux with

$$\begin{cases} \Phi_s^s = L_s i_s^s + L_m i_s^s \\ \Phi_r^s = L_r i_r^s + L_m i_r^s \end{cases} \quad (2)$$

The d and q axis rotor voltage equations (1a, 1b), and (2) in the synchronous rotating reference frame are given by

$$\begin{cases} V_{dr} = \frac{d\Phi_{dr}}{dt} - (\omega_s - \omega)\Phi_{qr} + R_r i_{dr} \\ V_{qr} = \frac{d\Phi_{qr}}{dt} + (\omega_s - \omega)\Phi_{dr} + R_r i_{qr} \end{cases} \quad (3)$$

The stator and rotor two axis fluxes are

$$\begin{cases}\Phi_{dr} = (L_{lr} + L_m)i_{dr} + L_m i_{ds} \\ \Phi_{qr} = (L_{lr} + L_m)i_{qr} + L_m i_{qs} \\ \Phi_{ds} = (L_{ls} + L_m)i_{ds} + L_m i_{dr} \\ \Phi_{qs} = (L_{ls} + L_m)i_{qs} + L_m i_{qr}\end{cases} \quad (4)$$

where, $L_r = L_{lr} + L_m, L_s = L_{ls} + L_m, \omega_r = \omega_s - \omega$

By substituting equation (4) in (3) and by rearranging the terms, then

$$\begin{cases} V_{dr} = (R_r + \frac{dL_r'}{dt})i_{dr} - s\omega_s L_r' i_{qr} + \frac{L_m}{L_s}V_{ds} \\ V_{qr} = (R_r + \frac{dL_r'}{dt})i_{qr} + s\omega_s L_r' i_{dr} + \frac{L_m}{L_s}(V_{qs} - \omega\Phi_{ds}) \end{cases} \quad (5)$$

From literature, the torque equation can be written as

$T_e = K_p(\Phi_{qs}\Phi_{dr} - \Phi_{ds}\Phi_{qr})$ (6)

Where ω is rotor speed, $\omega_{\Phi s}$ is speed of stator flux, ω_s is synchronous speed. K_p is a constant of $1.5(n_p * L_m/(L_s L_r - L_m^2))$.

The GSC control circuit block diagram is shown in Fig. 1a and MATLAB/ SIMULINK model is shown in Fig. 1b. The block diagram the control circuit of RSC for enhancing performance for LVRT issues with block diagram is shown in Fig. 2a and MATLAB/ SIMULINK is shown in Fig.2b.

The above equation 5 is rewritten in terms of decoupled parameters and is designed for RSC controller as in equation 7.

$$\begin{cases} \sigma V_{dr} = \sigma L_r \frac{dI_{dr}}{dt} - \omega_s \Phi_{qr} + \frac{L_m}{L_s}\left(V_{ds} - R_s I_{ds} + \omega_1 \Phi_{qs}\right) \\ \sigma V_{qr} = \sigma L_r \frac{dI_{qr}}{dt} + \omega_s \Phi_{dr} - \frac{L_m}{L_s}(R_s I_{qs} + \omega_1 \Phi_{ds}) \end{cases} \quad (7)$$

In general, the rotor speed is ω_r and the synchronous speed of stator ω_s .But this synchronous frequency has to be changed from ω_s to a new synchronous speed value ω_s' as it is represented commonly by ω_1 . Under ideal conditions, reference stator d-axis flux Φ_d^* is zero and q-axis flux Φ_q^* is equal to the magnitude of stator flux $\Phi_s$for given back emf and rotor speed.

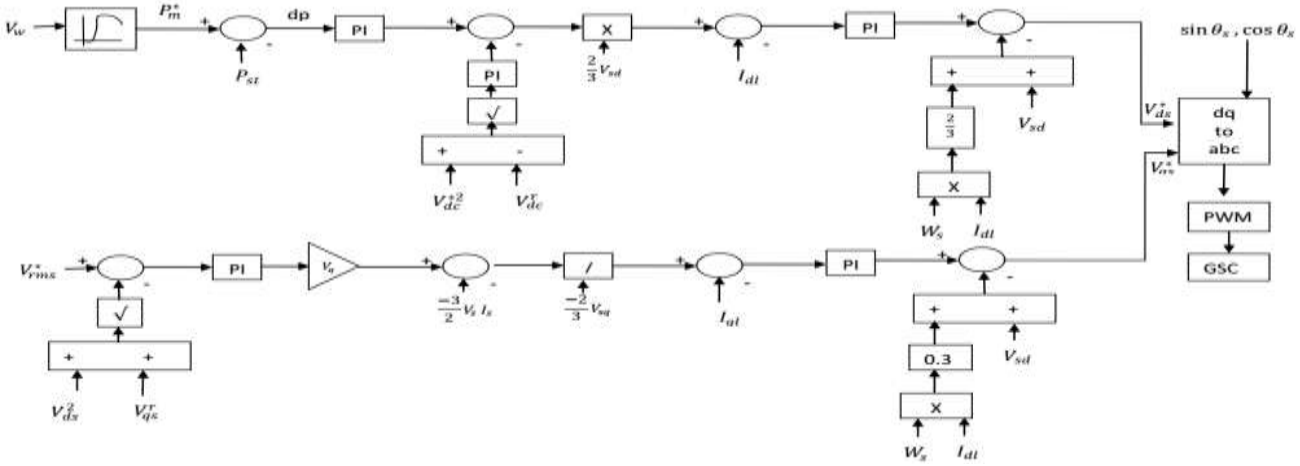

Fig.1a: Block diagram of GSC controller design for Grid connected DFIG

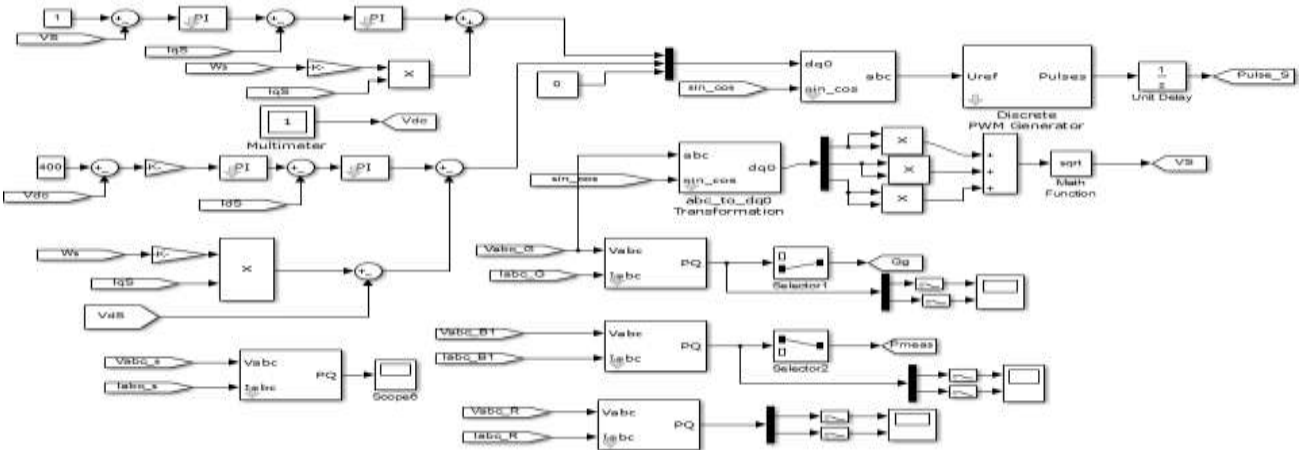

Fig.1b: MATLAB/ SIMULINK diagram of GSC controller design for Grid connected DFIG

The flux derivation technique helps in understanding the operation of DFIG during steady state and transient state. The accuracy of system performance during steady state depends on the accuracy of wind speed measurement action of pitch angle controller, measurement of stator current, voltage, flux and other important parameters. The more accurate these measurements, the more can be real power extracted from DFIG wind turbine system. The equations from 5 to 7 play a vital role in understanding the behavior of DFIG during steady state and accuracy of RSC control action depends on control of d and q axis voltages.

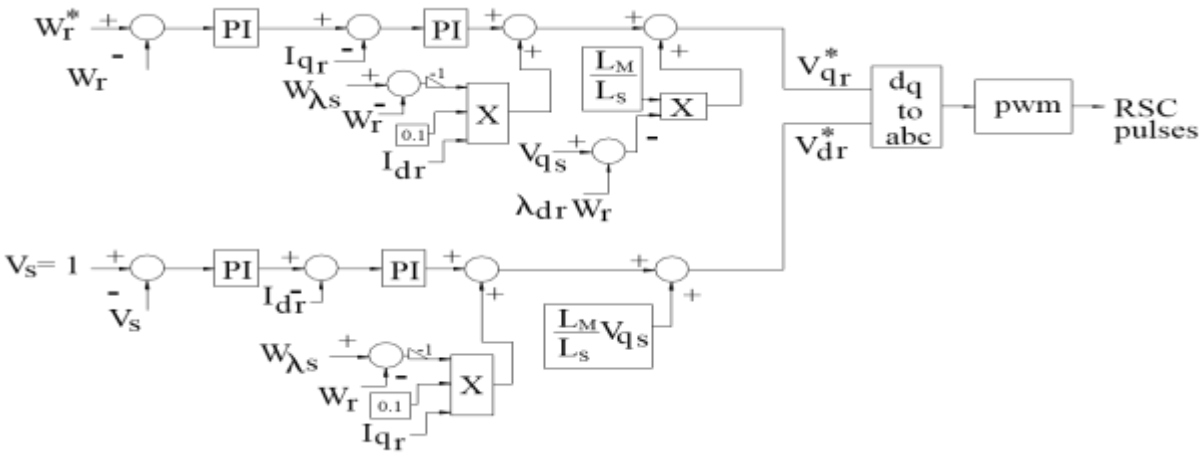

Fig.2a: block diagram of the RSC controller with EFOC technique design for Grid connected DFIG

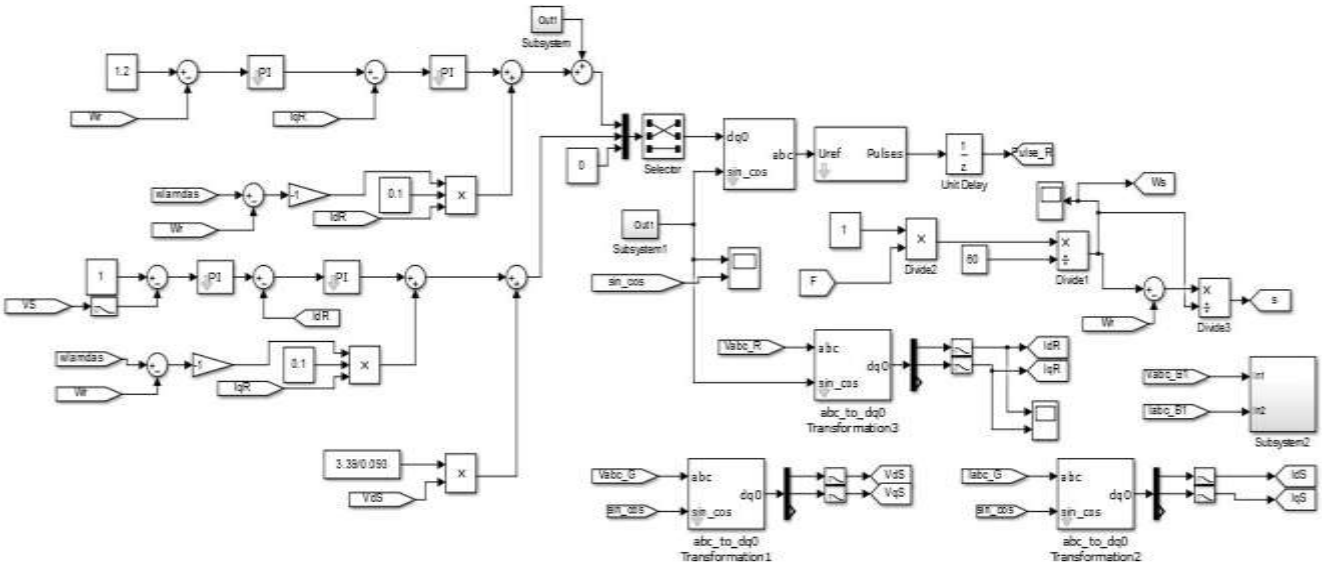

Fig.2b: MATLAB/ SIMULINK of RSC controller with EFOC technique design for Grid connected DFIG

2B Three Phase Symmetrical Faults

The stator voltage will reach zero magnitude during severe three phase's symmetrical fault of very low impedance and stator flux Φ_s gets reduced to zero magnitude. The decay in flux is not as rapid as in voltage and can be explained from the flux decay theorem available in literature and further can be explained as, delay is due to inertial time lag $\tau_s = \frac{L_s}{R_s}$ effecting the rotor induced Electromotive Force (EMF) V_{0r}. The flux during fault is given by

$$\Phi^s_{sf} = \Phi^s_s e^{-t/\tau_s} \quad (8)$$

and $\frac{d\Phi^s_{sf}}{dt}$ is negative, indicating its decay. By substituting (8) in (1b)

$$V^s_{0r} = -\frac{L_m}{L_s}\left(\frac{1}{\tau_s} + j\omega\right)\Phi^s_s e^{-t/\tau_s} \quad (9)$$

The above equation is converted into a rotor reference frame and neglecting $\frac{1}{\tau_s}$

$$V^s_{0r} = -\frac{L_m}{L_s}(j\omega)\Phi^s_s e^{-j\omega t} \quad (10)$$

By substituting $\Phi^s_s = \frac{V^s_s}{j\omega_s} e^{-j\omega_s t}$ in (20)

$$V^r_{0r} = -\frac{L_m}{L_s}(1-s)V_s \quad (11)$$

$|V^r_{0r}|$ is proportional to (1-s)

The converting equation (1a) into the rotor reference frame

$$V^r_r = V^r_{0r} e^{-j\omega t} + R_r i^r_r + \sigma L_r \frac{di^r_r}{dt} \quad (12)$$

A considerable decrease in pre-fault steady state voltage V^r_{0r} to certain fault voltage during a three phase fault was explained in above analytics. However, RSC converter is designed to meet V^r_r to match V^r_{0r} for rotor current control and the design has to be made for the rating of only 35% of stator rated voltage. The voltage dip during fault can be adopted independently or in coordination by using two techniques is explained below.

During the fault, at first instant, Φ_s does not fall instantly based on equation (4). If DFIG is running at super synchronous speed with slip (s) near to -0.2pu, during the

fault, rotor speed further increases based on the term (1-s) as given by (11).The above speed change is uncontrollable for a generator having higher electrical and mechanical inertia constants. In order to control the rotor current change, V_r^r has to be increased. Based on the first reason listed above, a voltage $V_{\Phi s}$ has to be injected in the feed forward path for improving the rotor dip to reach to its near steady state value. Converting the equation (7) into a synchronous reference frame and by considering direct alignment of Φ_{ds} with Φ_s we getting,

$$V_{\Phi s} = -\frac{L_m}{L_s}\omega\Phi_{ds} \quad (13)$$

The second technique for voltage increase requirement in a rotor is, dip can be compensated by replacing $s\omega_s$ with ($\omega_{\Phi s} - \omega$) in cross coupling terms $s\omega_s L_r' i_{qr}$ and $s\omega_s L_r' i_{dr}$ respectively. The reduction in magnitude and frequency of flux Φ_s, and alignment of flux with the stator voltage without the rate of change in flux angle $\theta_{\Phi s}$ indicates DC offset component in flux.

$$\frac{d\phi_s}{dt} = \omega_{\phi s} = 0 = \omega_f \quad (14a)$$

Here, $\omega_f$is the speed of stator flux during fault and this value can be made to zero as offset.

The voltage injection components shown in (12, 13) and compensating components (14a) as discussed above are estimated using enhanced flux oriented control (EFOC scheme RSC circuit shown in Fig.2 and the determined values are incorporated in the RSC controller.

$$\frac{d\theta_{\phi s}}{dt} = \omega_{\phi s} = \frac{V_{\beta s}\phi_{\alpha s} - V_{\alpha s}\phi_{\beta s}}{\phi_{\alpha s}^2 + \phi_{\beta s}^2} = \omega_f \quad (14b)$$

When dynamic stability has to be improved, proposed technique controls the decrease in stator and rotor flux magnitude and also damps oscillations at the fault instances. To achieve better performance during transients, this paper proposes a strategy for stator frequency reference to change to zero or other value depending on type and severity of disturbance. The accurate measurement of stator and rotor parameters like flux, current helps in achieving better performance during transients. The DC offset stator current reduction during transients and making the two-axis flux and voltage trajectories circular also improves the efficacy of the system performance during any faults. The equations 4 to 8 helps in understanding DFIG behavior during transient conditions and accuracy of its working depends on the measurement of rotor current and flux parameters.

The GSC controller design in MATLAB is shown in Fig. 1b. For particular wind speed, reference or optimal mechanical power from the turbine is estimated using a characteristic lookup table. The stator real power (P_{stator}) is measured and power error is the difference between these two powers (dP) which has to be maintained to zero using a PI controller. The PI output is then multiplied to the real power constant (K_p) gives actual power to be controlled after disturbance. The change in the square of the reference capacitor voltage DC link (V_{dc}^*) and square of actual capacitor voltage (V_{dc}) is controlled by the PI controller for reference controllable real power. The change in reference to actual controllable power is divided with $2/3V_{sd}$ to get d-axis current near grid terminal (I_{gdref}). Change in I_{gdref}^* and actual grid current I_{gdref} is controlled by PI to get d-axis voltage. For a better response during the transient state, decoupled d-axis voltage is added as done for separately excited DC motor control methodology. The decoupling helps in improving steady state error and tie up the transient response of DFIG during LVRT or when sudden real or reactive power changes to or from the system.

In the same way generally stator voltage (V_s^*=1) or reference reactive power (Q_s^*=0), actual stator voltage Vs or reactive power Q_s is decreased by the PI controller and multiplied with the reactive power constant (K_q) for actual reference reactive power recompense parameter. From the equation (21), actual reactive power is designed and this difference and actual reactive power compensating terms and dividing with $2/3V_{sq}$, to get q-axis reference current (I_{qref}). The difference in I_{qref} and I_q is controlled using PI to get reference q-axis voltage. To improve the transient response quickly and to minimize steady state error decoupled q-axis voltage to be added. Both d and q axis voltage so obtained are converted to three axis 'abc' parameters with inverse Park's transformation and this voltage is given to the PWM controller for grid side controller pulse generation.

3. DESIGN OF CONTROL CIRCUIT FOR STATCOM

The DFIG control circuits are shown in Fig.3 and the interconnected grid with coordinated three levels STATCOM is shown in Fig. 4. The background of the design of STATCOM controller with dynamic control of STATCOM ac and dc voltage, ac current with the design choice of an inductor is described here. The outer control loop is designed for control of real and reactive power flow, while inner control loop is with the current control loop for final dc and ac voltage control of STATCOM with PWM controller. The proposed topology shares the common dc link voltage across the capacitor of the back to back converters of DFIG. As the converters for DFIG is of low rating, the compensation of reactive power and stability can be improved using this coordinated STATCOM. The advantage of three levels STATCOM is, a more sinusoidal current waveform can be injected at the PCC compared to a two level one. The STATCOM control strategy is shown in Fig.5. The three level STATCOM current injection and ac and dc voltage control equations are derived as follows. The source voltage V_{sabc} in terms of STATCOM current i_{abc} and dc voltage across the three levels STATCOM capacitor V_{dc} is given below.

$$V_{sabc} = -Ri_{abc} + V_{dc}M_{abc} - L\frac{di_{abc}}{dt} \quad (15a)$$

In this, R and L are resistance and capacitance of coupling inductor of STATCOM and M_{abc} is duty cycle modulation index. The equation (15a) is represented in terms of dynamic injecting current as

$$\frac{di_{sabc}}{dt} = \frac{-Ri_{abc}}{L} - \frac{V_{sabc}}{L} + \frac{V_{dc}M_{abc}}{L} \quad (15b)$$

The dynamic equation in rotating 2 axis d and q axis reference frame of equation (15B)

$$\frac{di_d}{dt} = \frac{-Ri_d}{L} + \omega i_q - \frac{V_{sd}}{L} + \frac{V_{dc}M_d}{L} \quad (16a)$$

$$\frac{di_q}{dt} = \frac{-Ri_q}{L} + \omega i_d - \frac{Vs_q}{L} + \frac{V_{dc}M_q}{L} \quad (16b)$$

where id and iq are direct (d) axis and quadrature (q) axis currents of STATCOM. Similarly M_d and M_q are d and q axis modulation parameters of STATCOM which describe the switching period of VSC. The dq axis current can be simply written as

$$i_{dq}^* = \frac{G_1(s)G_2(s)}{1+G_1(s)G_2(s)}, \quad (17)$$

where $G_1(s) = K_{dq} + \frac{1}{s*\tau_{dq}}$ and $G_2(s) = \frac{1}{s+\frac{R}{L}}$

The reference d and q axis currents i_d^* and i_q^* can be written as and equivalent circuit control is in Fig.3. This is the inner and faster control loop control design of STATCOM

$$i_d^* = PI(V_{dc}^* - V_{dc}) = K_p(V_{dc}^* - V_{dc}) + K_i\int(V_{dc}^* - V_{dc})dt \quad (18a)$$

$$i_d^* = (V_{dc}^* - V_{dc}) * G_3(s) * G_4(s) \quad (18b)$$

$$i_q^* = (V_1^* - V_1) * G_5(s) * G_6(s) \quad (18c)$$

where $G_3(s) = K_{dc} + \frac{1}{s*\tau_d}$ and

$$G4(s) = \frac{K_d\tau_{ds}+1}{s^2\tau_d + s(K_d + \frac{R}{L})\tau_d + 1}$$

and $G_5(s) = K_q + \frac{1}{s*\tau_q}$ and

$$G_6(s) = \frac{K_q\tau_q s+1}{s^2\tau_q + s(K_q + \frac{R}{L})\tau_q + 1}$$

The PI represents proportional and integral controller for closed loop system with the constants K_p and K_i tuned using pole placement or trial and error method based on the designer's expertise in tuning PI controller. The dc, d and q axis proportionality constants are K_{dc}, K_d, K_q and time dc, d and q axis constants are τ_{dq}, τ_d and τ_q. The STATCOM controlled voltage in terms of d and q parameters are

$$V_{id} = L\left(K_p(i_d^* - i_d) + K_i\int(i_d^* - i_d)dt\right) - \omega L i_q + V_{sd} \quad (19a)$$

$$V_{i_q} = L\left(K_p(i_q^* - i_q) + K_i\int(i_q^* - i_q)dt\right) - \omega L i_d + V_{sq} \quad (19b)$$

The dynamic dc voltage across three level STATCOM VSC and the choice of ac side coupling inductor design is given below

$$\frac{dV_{dc}}{dt} = \frac{-3V_{dc}}{C_{dc}R_{dc}} - \frac{i_d M_d}{3} - \frac{i_q M_q}{3} \quad (20)$$

$$X_{acpu} = \frac{M_{\max} - M_{sb}}{M_{sb}} \quad (21)$$

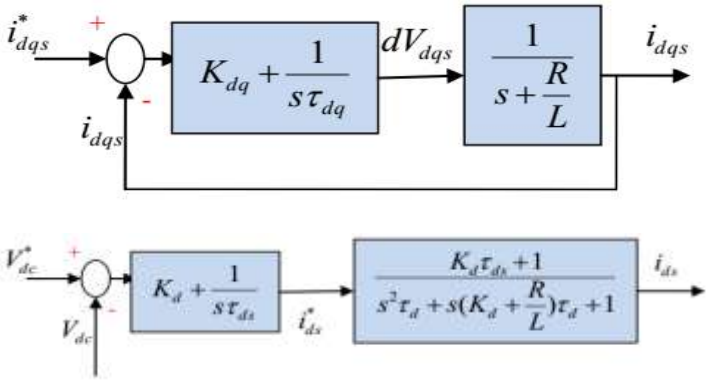

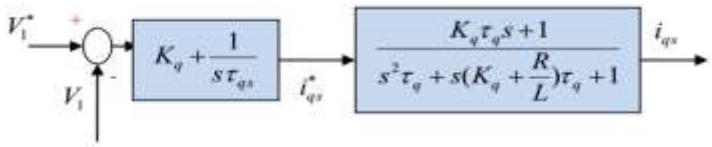

Fig.3. equivalent circuits of current and voltage controllers

The controller works on the principle of *PQ* control theory. The reference voltage and current are taken from PCC where reference real and reactive powers are extracted. Using 1st order transfer function model, direct and quadrature axis currents are derived from real and reactive powers. The instantaneous real and reactive powers can be expressed

$$\begin{cases} P = V_a i_a + V_b i_b + V_c i_c \\ Q = \frac{[(V_a - V_b) i_c + (V_b - V_c) i_a + (V_c - V_a) i_b]}{\sqrt{3}} \end{cases} \quad (22)$$

In two dimensional frames, the above equations can be represented as

$$\begin{cases} P = V_{gd} i_{gr\_d} + V_{gq} i_{gr\_q} \\ Q = V_{gq} i_{gr\_d} - V_{gd} i_{gr\_q} \end{cases} \quad (23)$$

In matrix form the two equations can be written as

$$\begin{bmatrix} P \\ Q \end{bmatrix} = \begin{bmatrix} V_{gd} & V_{gq} \\ -V_{gq} & V_{gd} \end{bmatrix} \begin{bmatrix} i_d \\ i_q \end{bmatrix} \quad (24)$$

$$Or \begin{bmatrix} i_{gr\_d} \\ i_{gr\_q} \end{bmatrix} = \frac{1}{V_{gd}^2 + V_{gq}^2} \begin{bmatrix} V_{gd} & -V_{gq} \\ V_{gq} & V_{gd} \end{bmatrix} \begin{bmatrix} P \\ Q \end{bmatrix} \quad (25)$$

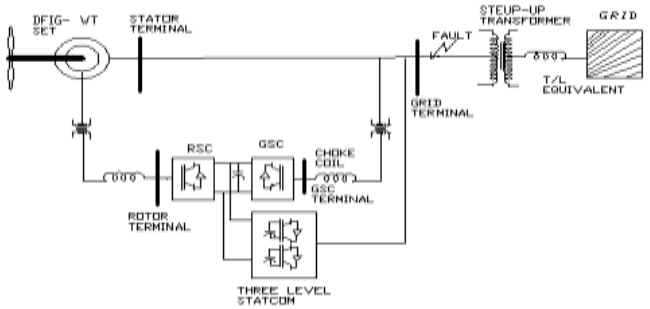

Fig.4. Grid connected DFIG with coordinated STATCOM

By substituting the values of reference voltages and powers, a first order transfer function can be obtained. This transfer function helps in extracting reference d and q axis currents. If there is a deviation in these reference currents, STATCOM will inject or absorb current to or from the system. In this Fig. 5, X is reactance and K is the instantaneous value of the voltage of STATCOM, E is the voltage at reference bus, V_d and V_q are direct and quadrature components of STATCOM. The transfer function is used to convert current to voltage parameters. Hence reference d and q axis reference voltage are derived. These d and q axis voltages are converted to three phase by using inverse Park's transformation with the help of phase locked loop (PLL). Based on equation (13), voltage in capacitor is converted to current by STATCOM. In this equation α refers to voltage angle at STATCOM bus and θ_s is phase angle produced by PLL.

If the feedback is positive, STATCOM will inject current, else will absorb current from the system. The energy stored in DC link capacitor is used for injecting current into the system. These three phase voltages are given to PWM pulse generator to generate pulses to the IGBT module. Thereby voltage at reference bus can be maintained constant.

The DFIG wind turbine system layout with STATCOM connected at Point of Common Coupling (PCC). Pitch controller is used to extracting maximum power from wind turbine during steady state by adjusting turbine blade angles and referring optimal rotor speed to Rotor side Converter (RSC) RSC controller. The STATCOM will inject current at required phase angle to compensate real and reactive power. The role of RSC, GSC was explained in brief in the next section.

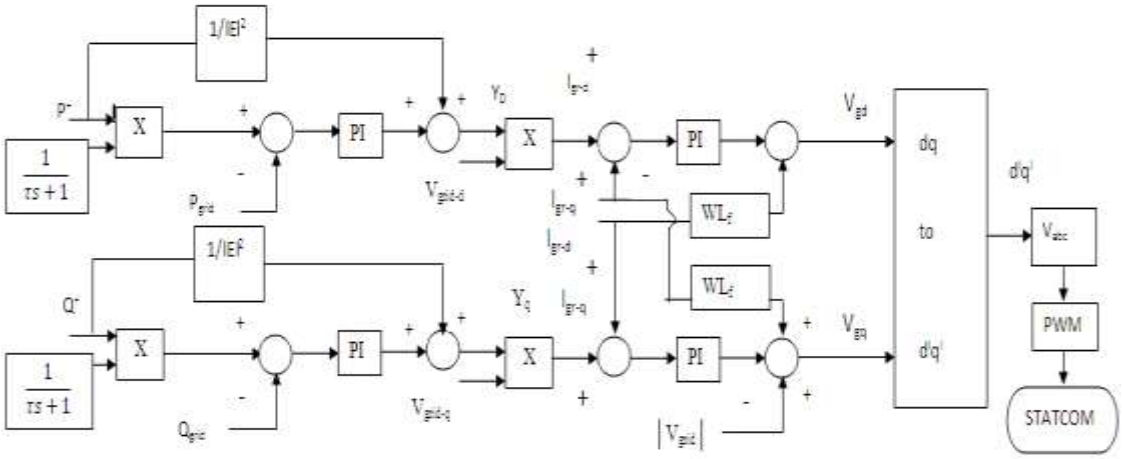

Fig.5. Block Diagram of three levels STATCOM controller

4. Result Analysis

In this, a general system was considered as shown in Fig.3. The DFIG is driven by a wind turbine and electric power from the generator is pumped to the grid for meeting a different loads requirement. The RSC is designed with EFOC technique to enhance operation during grid fault and has better dynamic stability features than a conventional FOC [6]. The role of RSC is to extract maximum power from the wind turbine, so the generator is made to rotate at that optimal speed by adjusting gear wheels between generator and turbine shaft. Another role of RSC is to improve the reactive power requirement during any abnormal situations like faults. The excess reactive power is supplied by RSC using the capacitor bank at RSC end and accuracy and fastness depend on the control strategy.

The GSC of DFIG has two main functions. One function is to maintain nearly constant voltage profile at DC link capacitor so that voltage at the point of common coupling (PCC) will also have a same value. The other function is to supply or absorb rapidly required reactive power. The GSC is also designed to bypass surge current to the converter terminal and stored in capacitor bank and to re-inject the excess power when fault gets relieved. In doing so, the fault current will not reach stator and from there to the rotor and hence GSC will protect the generator two windings.

Since the GSC and RSC are designed to a nearly 35% rating of stator terminals, the capability of reactive support will not be very high. If an external device which can support reactive power can help in compensating voltage dip and can improve current flowing capability from the generator during grid. Hence for the external reactive power support, a STATCOM is used. There are three cases studied in this section in comparison without and with STATCOM and the cases is, case A- single line to ground fault (SLG fault), case B- double line to ground fault (DLG fault) and case A- triple line to ground fault (TLG fault) with faults occurring at PCC during 0.7 to 0.8 seconds. The results can be compared with [28, 5] without STATCOM and [15] with STATCOM.

Case- A: Single-phase to ground fault (SLG)

A single-phase to ground (SLG) fault on ‘A’ phase ocured at point of common coupling near grid terminal with fault resistance of 0.001Ω during 0.6-0.9 seconds for the test system considered as shown in the Fig.3. Due to the fault with low resistance, A phase current at terminals like rotor, stator, grid side converter (GSC) and at the grid were decreased and the waveforms without STATCOM and with proposed EFOC technique is shown in Fig.6a(i). Compared to previous techniques, stator and rotor currents are maintained at certain value with proposed technique. Initially without fault, rotor and other parameters are having value of 1per unit (pu) and during fault, there is an increase in current magnitude to 1.2pu and with harmonics, still maintaining nearly sine waveform. At stator terminal, fault phase current increased slightly to 1.1pu and healthy two phases current are nearly constant. Similarly GSC terminal injecting current in two healthy phases decreased to 0.6pu and the fault phase is constant. At grid terminal, healthy phase current is constant fault phase current decreased to small value at 0.3pu. For system in [28], these current waveforms decreases to a very small value and takes time to get settled after relieving from fault.

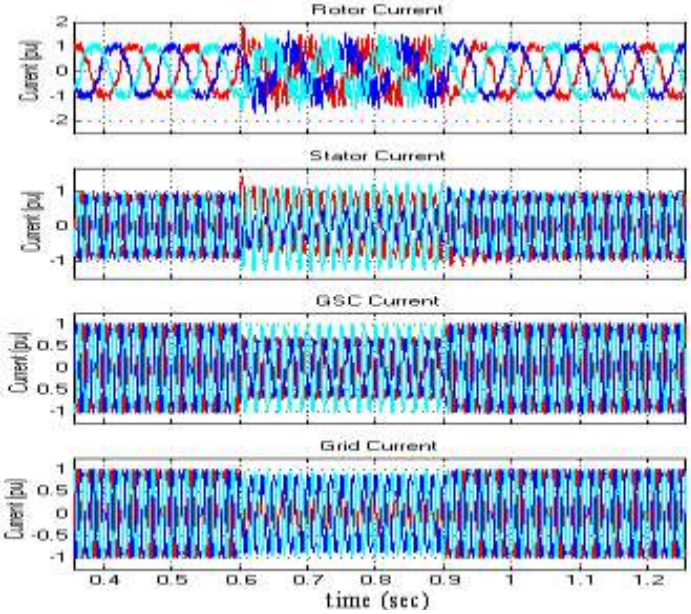

Fig. 6a (i) without STATCOM

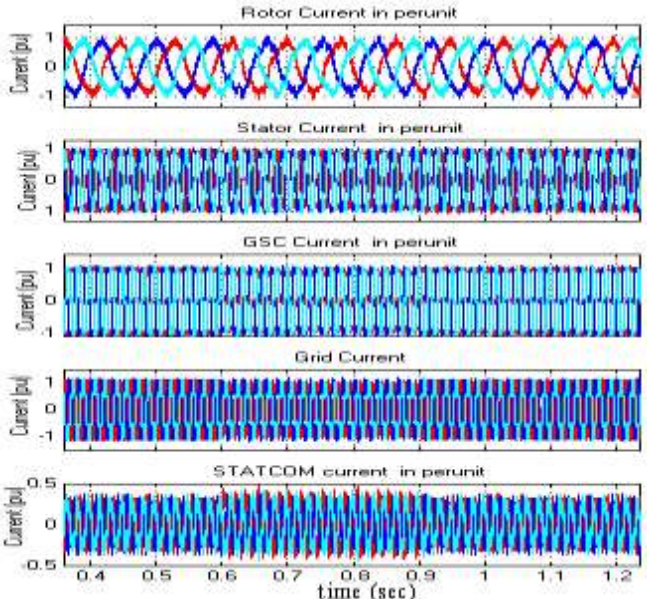

Fig. 6a (ii) with STATCOM

Fig.6a Rotor, stator GSC and grid terminal current waveforms with EFOC technique with SLG fault

With the aid to proposed control EFOC strategy, a three level STATCOM is in coordination with the present system to improve LVRT issue for grid connected DFIG system during the severe disturbance. It can be observed that with three levels STATCOM, all the terminal currents like the rotor, stator and grid converter and at grid terminal are maintained constant during and after the fault as shown in Fig.6a (ii). The STATCOM current that phase increased to 0.45pu from0.4pu to compensate the decrease in current and to supply reactive power during the fault.

The DC capacitor voltage in volts and rotor speed and torque in pu without STATOM and with STATCOM are shown in Fig.6b. Without STATCOM, the DC link voltage decreased from 830 volts to 800 volts during fault and then increased to 835V at the instant after fault and maintained the same 830V from then. The rotor speed with an initial value of 1.95pu increased to 1.21pu during fault and then reached to 1.2pu and maintained constant with the EFOC technique without STATCOM as in Fig.6b(i). The torque output from generator has ripples during fault and changed its value from -0.8pu to average of 0.5pu during fault and reaches its pre-fault value immediately after the fault was cleared.

In the same system with the same fault but with STATCOM as in Fig.6b (ii), the DC link voltage at back-to-back converters of DFIG was maintained constant at 800 volts during and after the fault. This is due to the fast action of STATCOM for reactive support and also because of higher rating of STATCOM DC capacitor values.

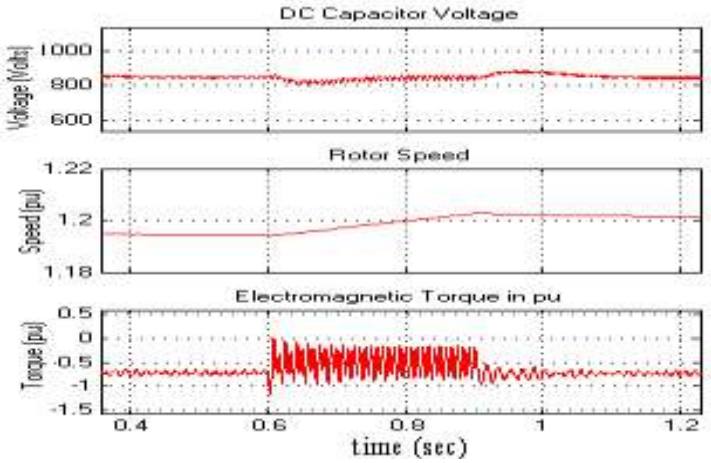

Fig. 6b (i) without STATCOM

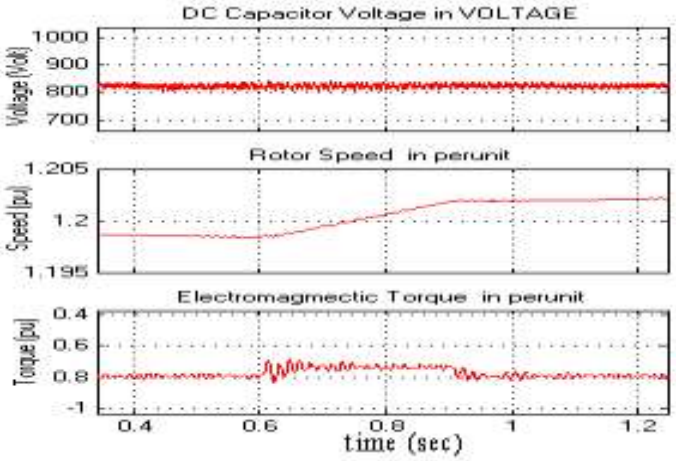

Fig. 6b (ii) with STATCOM

Fig.6b DC capacitor voltage in volts and rotor speed and torque in pu waveforms with EFOC technique

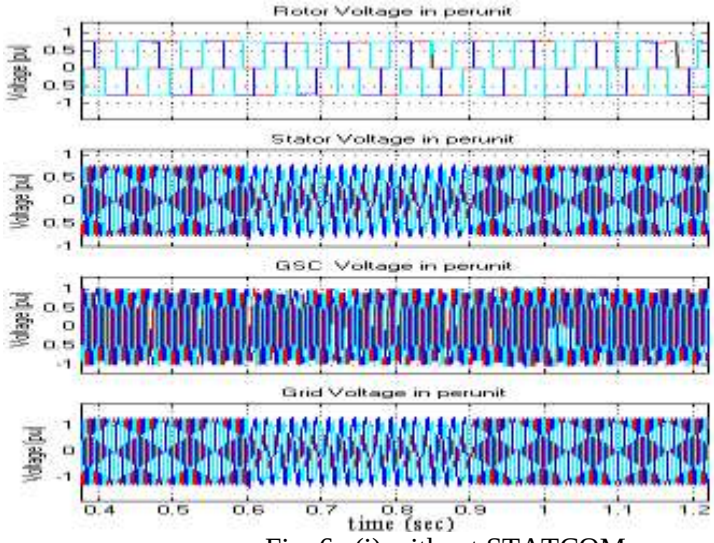

Fig. 6c (i) without STATCOM

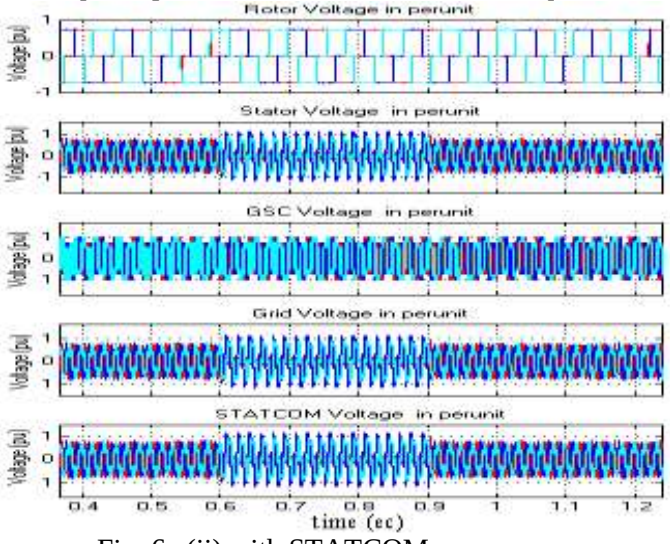

Fig. 6c (ii) with STATCOM

Fig.6c Rotor, stator GSC and grid terminal voltage waveforms with EFOC technique with SLG fault

The rotor speed has a very small change from 1.197 to 1.202pu during fault and can be said to be constant with STATCOM based system. The electromagnetic torque (EMT) of DFIG is initially at -0.8pu and decreased in magnitude to nearly 0.7pu with lesser ripples compared to the system without

STATCOM and also has better stabilization once fault was eliminated. The same system with SLG fault with a conventional controller will have large torque pulsations, uneven decrease during fault and surge voltage produced when the fault was cleared. However, with EFOC, the performance is better and is better with STATCOM.

The rotor terminal voltage, stator, grid side converter (GSC) and grid terminal voltages in pu without STATCOM and with STATCOM are shown in Fig. 6c. The rotor and GSC voltages are nearly constant without STATCOM as in Fig.6c (i) during and after the A-phase to ground fault. The fault occurred at grid terminal, so that phase voltage decreased while maintaining two healthy phases waveform remained nearly constant but with a small change in phase angles. Since stator is directly connected to the grid, the effect of fault will have an impact on the stator, but with proposed control scheme, the voltage still maintained at 0.45pu from 0.8pu. With conventional control scheme, it decreased to much lower value at 0.2pu without STATCOM.

The voltage waveforms for same parameters with STATCOM is shown in Fig.6c(ii). The rotor and GSC voltages are constant during and ate fault, the stator and grid terminal voltages changed during fault and the STATCOM voltage waveform changed. There were very fewer papers in the literature to study the machine and terminal voltage behavior during faults. Hence this paper will lay a small step towards the analysis and be understanding the voltage waveforms during and after the fault. For the STATCOM system, if passive filters were used, the waveforms will get much more sine waveforms.

Maintenance of stator and rotor voltage and current waveforms during and after faults helps in improving stability, reliability, performance and lifetime. Hence proposed EFOC technique can do so effectively meet recent grid codes and further the improvement was made with STATCOM. It can also be understandable that, asymmetrical faults results in large torque pulsations, deviation in rotor speed, flushing of large current harmonics in stator as well as rotor terminals and finally decrease in performance during faults.

Case- B: Double Line to Ground fault (DLG)

A two or double line to ground fault (DLG) between A-B and ground is expected to arrive at PCC during the same time from 0.6 to 0.9 seconds with same fault resistance of 0.001Ω is considered in this case study. This fault is more severe than SLG fault because of the decrease in voltage value in two phases. However, occurrence is lesser than SLG fault in practical systems. Due to the fault with the low resistance of 0.001Ω, A and B phases current at rotor, stator, grid side converter (GSC) and at the grid terminals decreased and the waveforms without STATCOM and with proposed EFOC technique shown in Fig.7a(i). Compared to previous techniques, stator and rotor currents are maintained at a certain value with proposed technique. Initially, without fault, rotor and other parameters are 1pu without fault and during the fault, there is an increase in current magnitude to 1.8pu in two phases (red and blue) and with harmonics, still maintaining nearly sine waveform. At stator terminal, fault phases current increased to 1.2pu and the healthy phase current decreased to 0.9pu. Similarly GSC terminal injecting current in all phases decreased to 0.5pu and during the fault. At grid terminal, healthy phase current decreased to 0.8pu during fault and the faulty phases current decreased to a value at 0.25pu. For a conventional system [28, 5], these current waveforms decrease to a very small value and take a time to get settled after relieving from fault.

With proposed EFOC strategy and a three level STATCOM, with the performance for LVRT issue for grid connected DFIG system during severe disturbance like DLG was analyzed. It can be observed that with three levels STATCOM, all the terminal currents like the rotor, stator and grid converter are maintained nearly constant during and after the fault as shown in Fig.7a (ii). The stator terminal current increased from 1pu to 1.1 at the instant of fault occurrence and reached steady state easily and even during the fault. The GSC terminal current in healthy phase is constant at 1pu and in faulty phases, it decreased to 0.5pu during DLG fault. The STATCOM injecting current the two phases increased to 0.55pu from 0.4pu to compensate the decrease in current and to supply reactive power during the fault.

The DC capacitor voltage in volts and rotor speed and torque in pu without STATOM and with STATCOM are shown in Fig.7b. Without STATCOM, the DC link voltage decreased from 830 volts to 780 volts during the instant of fault and increased to 910V at the instant after fault and reached steady state at 1.14s at 830V from then. The rotor speed with an initial value of 1.95pu increased to 1.21pu during fault and then reached to 1.2pu and maintained constant with the EFOC technique without STATCOM as in Fig.7b(i). The torque output from generator has ripples during fault and changed its value from -0.8pu to average of 0.25pu during the fault and reaches its pre-fault value immediately after the fault was cleared. The lowest value of torque pulsation surges is 0pu with variation up to -0.8pu during fault. The system with the same type of fault reaches to zero average value in Fig. 7b (ii) in [28]. Hence proposed system has better capability to withstand DLG faults also.

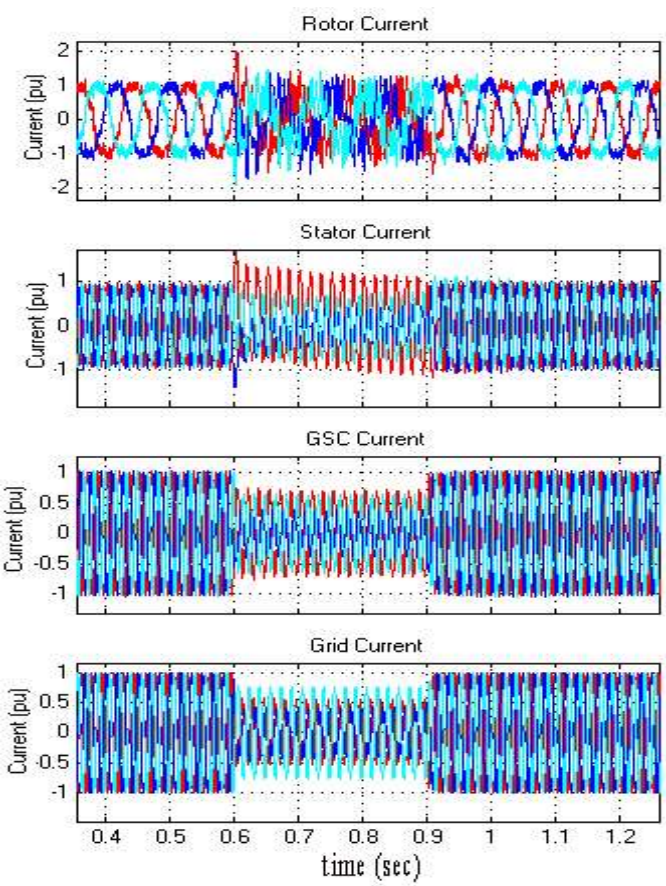

Fig. 7a (i) without STATCOM

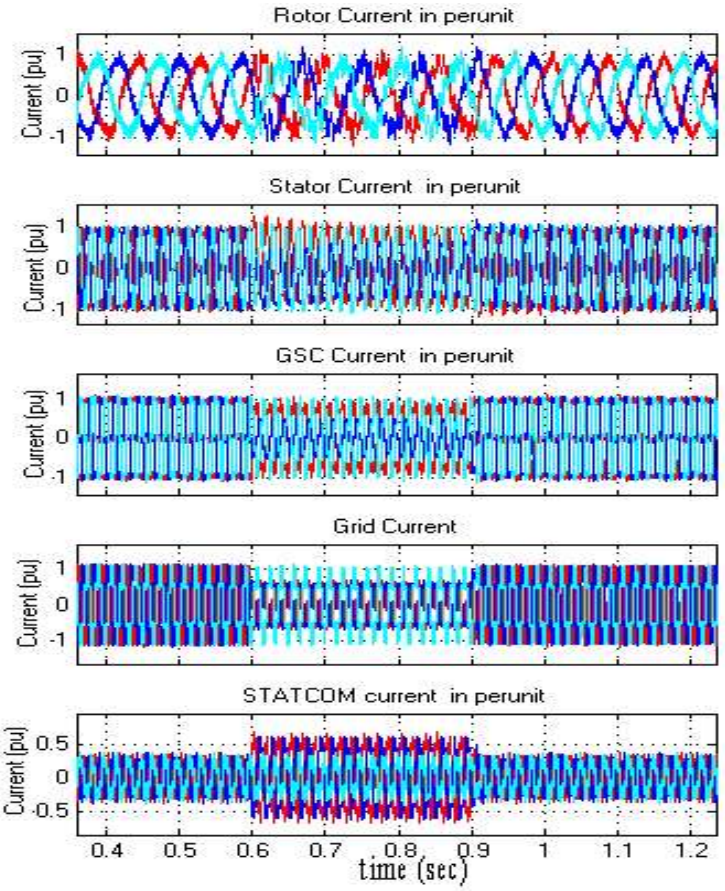

Fig. 7a (ii) with STATCOM

Fig.7a Rotor, stator GSC and grid terminal current waveforms with EFOC technique with DLG fault

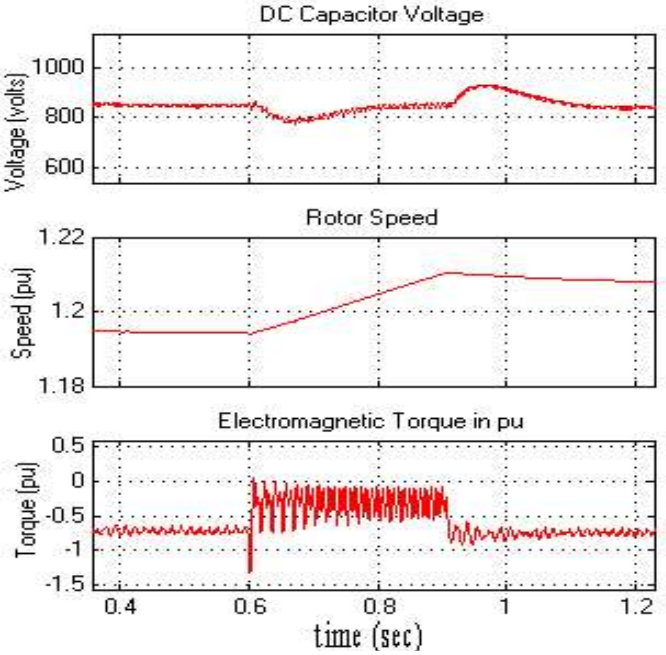

Fig. 7b (i) without STATCOM

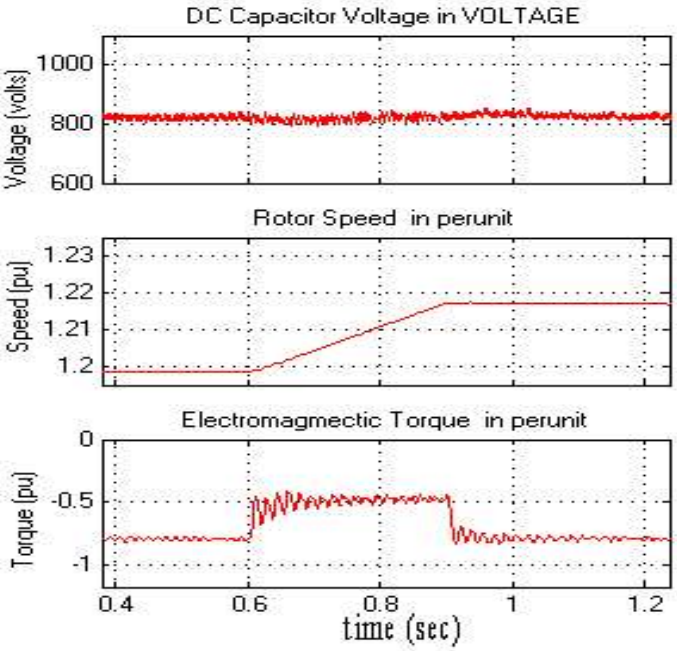

Fig. 7b (ii) with STATCOM

Fig.7b DC capacitor voltage in volts and rotor speed and torque in pu waveforms with EFOC technique

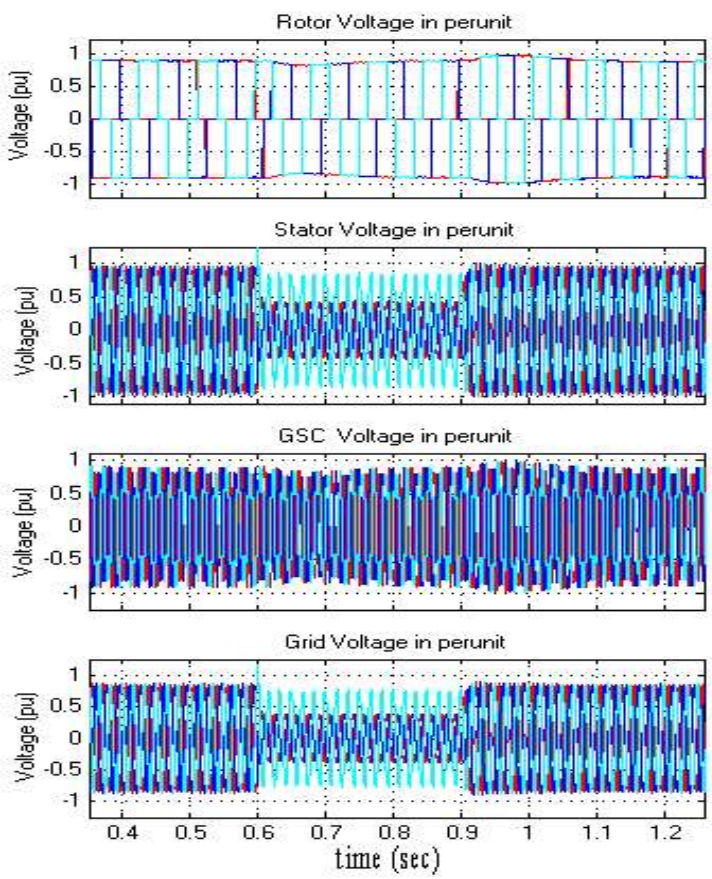

Fig. 7c (i) without STATCOM

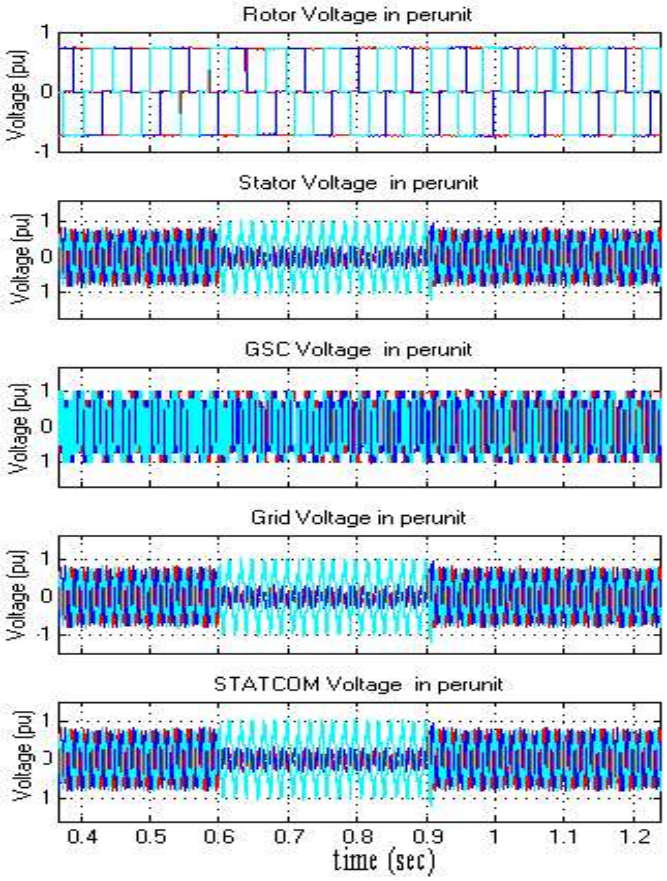

Fig. 7c (ii) with STATCOM

Fig.7c Rotor, stator GSC and grid terminal voltage waveforms with EFOC technique with DLG fault

For the same system with the same fault but with STATCOM as in Fig.7b (ii), the DC link voltage at back-to-back converters of DFIG was maintained constant at 800 volts during and after the fault. The rotor speed has a small change from 1.197 to 1.21pu during fault without STATCOM and to 1.22pu speed with STATCOM based system. The electromagnetic torque of DFIG which is initially at -0.8pu and decreased in magnitude to nearly -0.5pu with lesser ripples compared to a system without STATCOM and also has a quicker response once fault was cleared. The same system with DLG fault with a conventional controller in [28, 15] are having large torque pulsations with average zero torque value during fault and surge voltage produced at the instant when the fault was cleared. But with EFOC, the performance is better and is can be improved more effectively with three level STATCOM.

The rotor terminal voltage, stator, grid side converter (GSC) and grid terminal voltages in pu without STATCOM and with STATCOM are shown in Fig. 7c. The rotor and GSC voltages are nearly constant without STATCOM as in Fig.7c (i) during and after the A and B phases to ground fault. Since stator is directly connected to the grid, the effect of fault will have an impact on the stator, but with proposed control scheme, the stator voltage still maintained at 0.45pu from 0.8pu. With conventional control scheme, voltage decreased to much lower value at 0.2pu without the three level STATCOM. The compensation in voltage at different terminals without and with STATCOM is nearly same as in Fig.7c (ii). The introduction is to damp torque oscillations, control stator and rotor terminal currents and to improve real and reactive power flow from the generator to a grid so as meet desired load requirements effectively.

Case- C: Three-Lines to Ground fault (TLG) or symmetrical fault.

The most severe and rare occurrence of fault is Triple line to ground (TLG) fault. It is also called as symmetrical fault due to balanced (symmetrical) change in voltage and current waveforms. Depending on fault resistance the voltage and current at generator terminal decrease. For a very small resistance fault, the stator voltage and current sometimes reache zero magnitudes and results in very small flux and much increase in rotor speed during the fault. Mostly, relays protect the system from getting damaged, however, reliability will be lost. If the dynamic stability of DFIG is improved, it stays in

synchronism during and after the fault. For this EFOC is an excellent alternative.

The rotor and stator current waveform decreased from 1pu to 0.88pu and 0.65pu during fault without STATCOM as shown in Fig. 8a(i). Once fault was relieved, there is a faster stabilization in all three phases. A small sub-transient was observed in different phases at instants of fault occurrence and clearance.It is due to the residual voltage not being zero or high at that instants. So, there is an increase in sub-transient current those phases. The GSC terminal and grid terminal current were reduced to a very 0.4pu during fault due to the low resistance of ground to phases. For the same system with STATCOM, rotor current is improved a little compared to the system without STATCOM with a value of 0.92pu and much quicker stabilization of rotor current after the fault. The stator current is also at 0.9pu during fault and the magnitude of sub-transient currents are very low with STATCOM. The grid and GSC terminal currents remaining same at 0.4pu even with STATCOM as in Fig. 8a(ii). The STATCOM injecting current is from 0.5pu to 0.8pu during the fault, so as to compensate the dip in rotor and stator current referred at PCC.

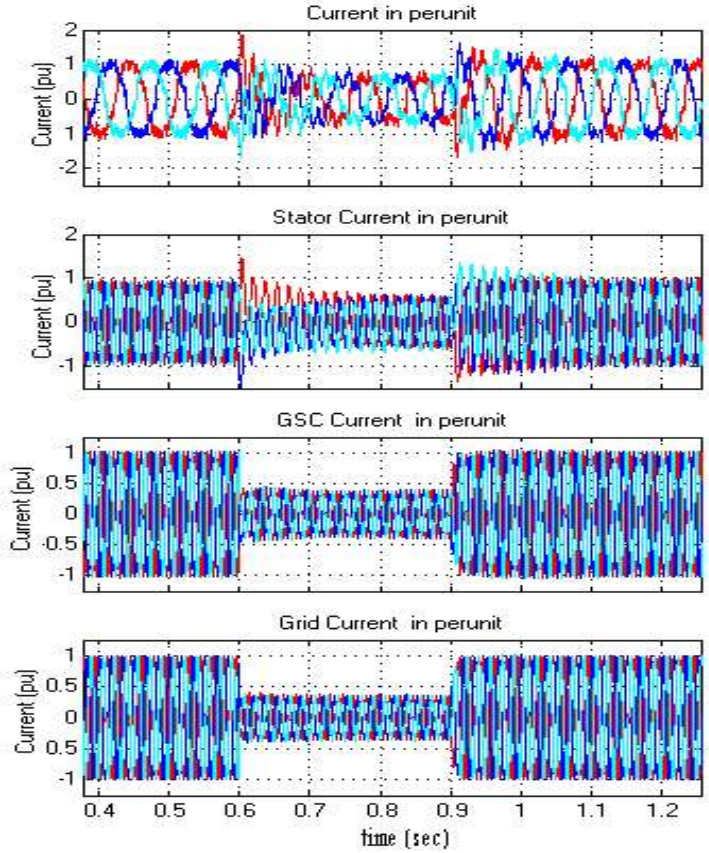

Fig. 8a (i) without STATCOM

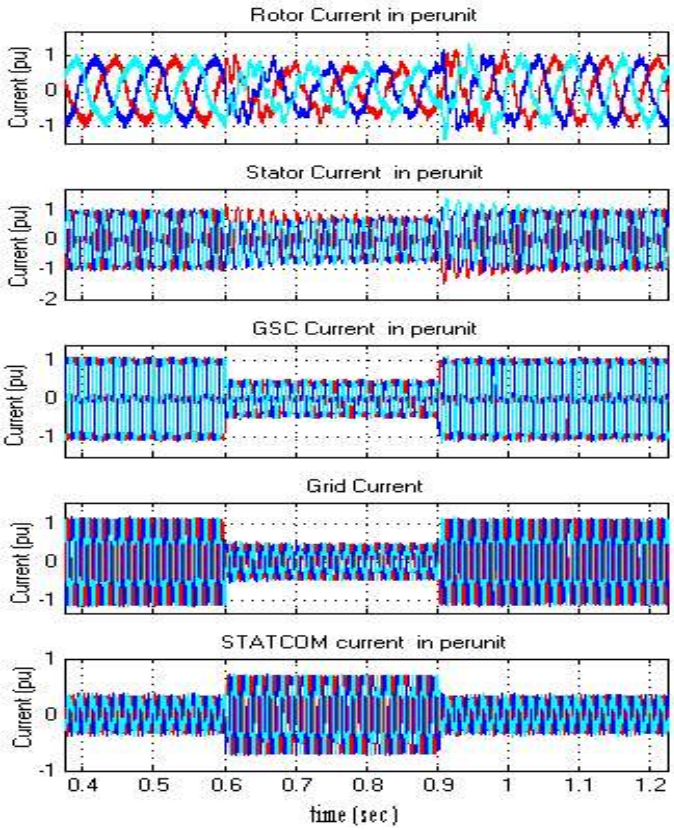

Fig. 8a (ii) with STATCOM

Fig.8a Rotor, stator GSC and grid terminal current waveforms with EFOC technique with TLG fault

The dc capacitor voltage in volts and rotor speed and torque in pu for a three phase to ground fault (TLG) at PCC without STATOM and with STATCOM are shown in Fig.7b. Without STATCOM controller, the DC link voltage decreased from 830 volts to 710 volts during the instant of fault and increased to 1000V at fault instant and reached steady state at 1.15s at 825V from then. The rotor speed with an initial value of 1.95pu increased to 1.218pu during the fault and then reached to 1.216pu and maintained nearly constant with the EFOC technique without STATCOM as in Fig.8b (i). The torque output from generator has ripples during fault and changed its value from -0.8pu to average of -0.15pu during the fault and reaches its pre-fault value in 1.14 seconds after the fault was cleared. The lowest value of torque pulsation surges is -0.05pu with variation up to -0.8pu during fault. Hence proposed system has better capability to withstand DLG faults also.

For the same system with the same fault but with STATCOM as is shown in Fig.8b (ii), the DC link voltage at back-to-back converters of DFIG was maintained constant at 800 volts during and after the fault. The rotor speed changed from 1.197 to 1.216pu during fault without STATCOM and to 1.226pu speed with STATCOM controller. The electromagnetic torque of DFIG which is initially at -0.8pu and decreased in magnitude to nearly -0.25pu with lesser ripples and settled at 1 second when the fault was cleared, compared

to the system without STATCOM and also has faster dynamic response during and after the fault. The same system having TLG fault in [5] are having large torque pulsations with average zero torque value during fault and surge voltage produced at the instant when the fault was cleared. But with EFOC, the performance is better and is can be improved more effectively with three level STATCOM.

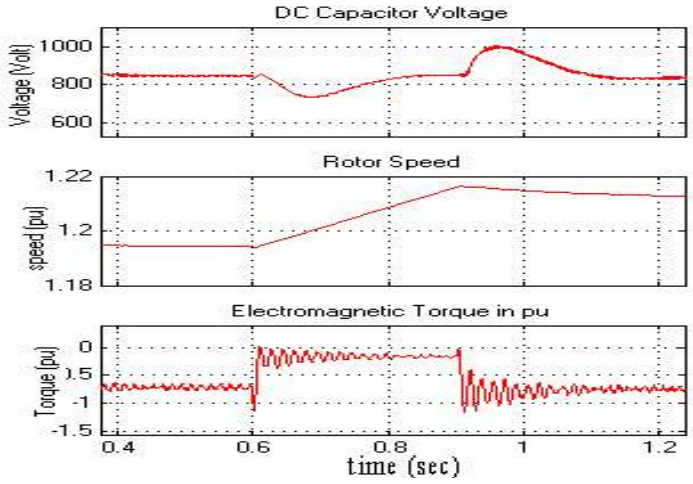

Fig. 8b (i) without STATCOM

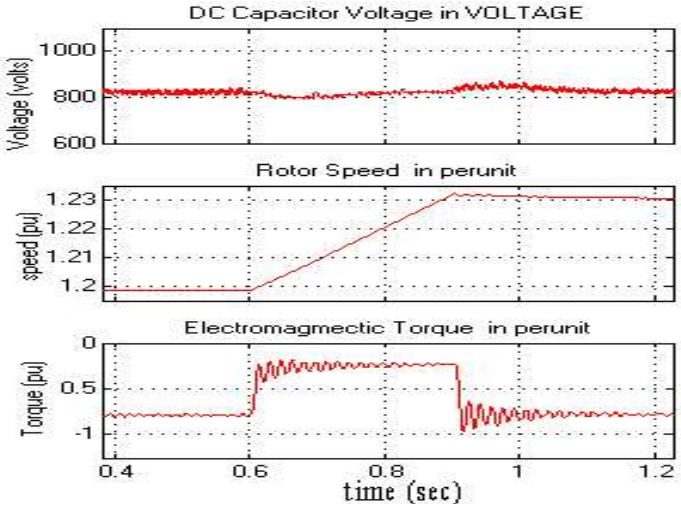

Fig. 8b (ii) with STATCOM

Fig.8b DC capacitor voltage in volts and rotor speed and torque in pu waveforms with EFOC technique

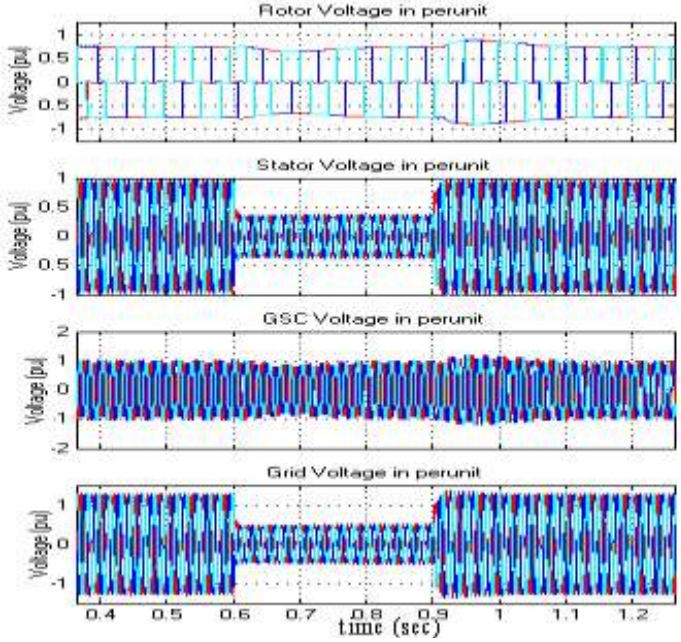

Fig. 8c (i) without STATCOM

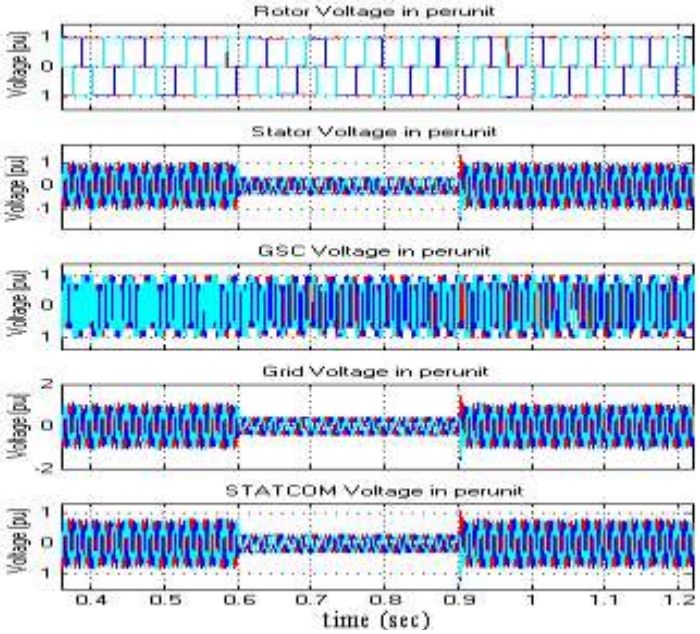

Fig. 8c (ii) with STATCOM

Fig.8c Rotor, stator GSC and grid terminal voltage waveforms with EFOC technique with TLG fault

The rotor terminal voltage, stator, grid side converter (GSC) and grid terminal voltages in pu without STATCOM and with STATCOM are shown in Fig. 8c. The rotor and GSC voltages are nearly constant without STATCOM as in Fig.8c (i) during and after the A -B phases to ground fault. With the proposed controller, the stator voltage still maintained at 0.45pu from 1pu as in Fig. 8c (ii).

The EFOC technique and STATCOM can operate effectively with both symmetrical plus asymmetric faults with rapid controlling action and much better performance during and after the fault. The dynamic and transient stability and also power transfer capability can be enhanced with the proposed system. The results presented in this paper are better than the results available in the literature [1, 9 and 13]. The stator and rotor currents are less than 2pu during faults, torque is not reaching zero and oscillations died quickly. Speed increase during faults is very low, DC capacitor voltage rise during and after the fault clearing is also very much within limits with proposed coordinated three level STATCOM strategy compared to the literature.

5. Results Discussion

A conventional DFIG system connected to the grid was considered and three different cases of faults are analyzed

without and with three level STATCOM. The three cases are an asymmetric fault (SLG, DLG) and symmetric fault (TLG) faults taken place at PCC during 0.6 and 0.9 seconds with fault resistance of 0.001 ohms. The drop in rotor terminal current during any type of fault remained nearly constant during fault during asymmetric faults and stator current dropped to half during the symmetric fault and maintained near to 75% current magnitude in stator during DLG fault. With proposed EFOC technique, rotor current in any case of a fault is not getting to zero value, but stator current decreased as it is directly connected to the grid and has higher impact during grid symmetric faults. With the three level STATCOM, the drop in rotor current was minimized, DC link voltage at back-to-back of DFIG converters was maintained constant, electromagnetic torque drop and pulsations were controlled. Stator terminal current was limited to half value from not getting to zero during a severe grid fault. The grid voltage and current decreased to a less than half the value during symmetric fault and half of its pre-fault value for asymmetric fault during fault without STATCOM and can be recovered from falling by using STATCOM.

In all the cases, rotor speed remained constant from being deviation during the fault. The drop in DC link voltage at back to back converters of DFIG increases with increase in phases to ground fault and also post-fault recovery takes place with a small surge in voltage. The decrease in DC link voltage can be minimized and hence PCC voltage can be improved by using STATCOM. The electromagnetic torque output from DFIG is having more oscillations and reaches slowly to steady state with asymmetric faults than with symmetric faults due to symmetric decrease in flux value and recovers very rapidly without fluctuations. With proposed EFOC control strategy with coordinated STATCOM, there is a much better compensation in stator and rotor voltage and current compared to literature. The damping of EMT during the fault is better and it is not getting to zero Nm or lower magnitude value with proposed control scheme. The rotor speed is also within limits and maintained at a particular speed during the fault. Whereas in the conventional technique, EMT will have high-frequency oscillations with speed go on increasing during the faut. The dacay in the flux is also controlled by not going to decay much further, is achieved by changing the reference synchronous speed value as described in the flow chart. The above all are the major contributions to the proposed strategy.

The post-fault recovery in machine voltage and current took place with small surges in voltage. The decrease in DC link voltage are minimized and hence PCC voltage was improved using EFOC technique with FC. The electromagnetic torque output from DFIG have fewer oscillations and reached immediately to steady state even during faults and also after fault clearing. There are few surges in torque and current at starting and clearing of faults. It is due to a symmetric decrease in flux value and with the proposed EFOC it recovers very rapidly without any fluctuations.

6. Conclusion

With conventional control scheme, voltage decreased to much lower value at 0.5pu without STATCOM. The compensation in voltage at different terminals without and with STATCOM is nearly same. The introduction is to damp torque oscillations, control stator and rotor terminal currents and to improve real and reactive power flow from the generator to the grid so as meet desired load requirements effectively. With proposed EFOC control strategy, there is a much better compensation in stator and rotor voltage and current compared to literature. The damping of EMT during the fault is better and it is not getting to zero Nm or lower magnitude value with proposed control scheme. The rotor speed is also within limits and maintained at a particular speed during the fault. Whereas in a conventional technique, EMT will have high-frequency oscillations with speed go on increasing during the faut. The main advantages of this method is DC offset current components are minimized to very small quantity and oscillations in torque and speed are also damped quickly. The stator and rotor currents are non- zero or huge values during any type of fault.

The DC offset of flux is also controlled by proposed system. In the system designed for both with LVRT, stator and rotor current decays to a very small value such that reaching its pre-fault after clearing the fault takes more time for a conventional system. But for our system, stator and rotor currents remain almost constant for 50% dip in grid voltage. The post-fault recovery in machine voltage and current are taken place with small surges in voltage. The decrease in DC link voltage is minimized and hence PCC voltage was improved using EFOC technique.

Thus our proposed system will follow modern grid codes very easily and even can be suitable for very harsh over voltage system. It does not require any additional reactive power sources like FACTS devices or energy storage devices. A conventional controller like PI with fast acting relay and converters are needed for RSC and GSC to enhance the system behavior during HVRT for proposed EFOC technique. With proposed EFOC control strategy, there is a much better compensation in stator and rotor voltage and current compared to literature. The damping of EMT during the fault is better and it is not getting to zero Nm magnitude value with proposed control scheme. The rotor speed is also within limits and maintained at a particular speed during the fault.

The decay in the flux is also controlled by not going to decay much further, is achieved by changing the reference synchronous speed value as described in the flow

chart. The above all are the major contributions to the proposed strategy.

APPENDIX

The parameters of DFIG used in simulation are,
Rated Power = 1.5MW, Rated Voltage = 690V, Stator Resistance Rs = 0.0049pu, rotor Resistance Rrl = 0.0049pu, Stator Leakage Inductance Lls = 0.093pu, Rotor Leakage inductance Llr1 = 0.1pu, Inertia constant = 4.54pu, Number of poles = 4, Mutual Inductance Lm = 3.39 pu, DC link Voltage = 415V, Dc link capacitance = 0.2F, Wind speed = 14 m/sec.
Grid Voltage = 25 KV, Grid frequency = 60 Hz.
Grid side Filter: Rfg = 0.3Ω, Lfg = 0.6nH
Rotor side filter: Rfr = 0.3mΩ, Lfr = 0.6nH
STATCOM: capacitance= 0.1F, transformer-690/440V, 50kVA rating, PWM frequency=2kHz.

References

[1] Wang Yun ; Zhao Dong-li ; Zhao Bin ; Xu Hong-hua, "A Review of Research Status on LVRT Technology in Doubly-fed Wind Turbine Generator System", Proc. on ICECE, 2010, pp: 4948 – 4953.

[2] Shuai Xiao ; Hua Geng ; Honglin Zhou ; Geng Yang, "Analysis of the control limit for rotor-side converter of doubly fed induction generator-based wind energy conversion system under various voltage dips", IET Renewable Power Generation, , Volume: 7, 2013 , pp: 71 – 81

[3] Shuai Xiao ; Geng Yang ; Honglin Zhou ; Hua Geng,"An LVRT Control Strategy Based on Flux Linkage Tracking for DFIG-Based WECS",, IEEE Transactions on Industrial Electronics, Volume: 60 , Issue: 7, 2013 , Pp: 2820 – 2832

[4] Dong liang Xie ; Zhao Xu ; Lihui Yang ; Ostergaard, J. ; Yusheng Xue ; Kit Po Wong, "A Comprehensive LVRT Control Strategy for DFIG Wind Turbines With Enhanced Reactive Power Support", IEEE Transactions on Power Systems, Volume: 28 ,2013 , pp: 3302 – 3310

[5] Lihui Yang ; Zhao Xu ; Ostergaard, J. ; Zhao Yang Dong ; Kit Po Wong, "Advanced Control Strategy of DFIG Wind Turbines for Power System Fault Ride Through," IEEE Transactions on Power Systems, Volume: 27 , Issue: 2,2012 , Pp: 713 – 722

[6] Rahimi, M. ; Parniani, M., "Efficient control scheme of wind turbines with doubly fed induction generators for low-voltage ride-through capability enhancement", IET Renewable Power Generation, Volume: 4 , Issue: 3,2010 , pp: 242 – 252

[7] Jiaqi Liang ; Howard, D.F. ; Restrepo, J.A. ; Harley, R.G., "Feedforward Transient Compensation Control for DFIG Wind Turbines During Both Balanced and Unbalanced Grid Disturbances" IEEE Transactions on Industry Applications, Volume: 49 , Issue: 3, 2013 , pp: 1452 – 1463

[8] Jiaqi Liang ; Wei Qiao ; Harley, R.G., "Feed-Forward Transient Current Control for Low-Voltage Ride-Through Enhancement of DFIG Wind Turbines", IEEE Transactions on Energy Conversion, Volume: 25 , Issue: 3, 2010 , pp: 836 – 843

[9] Vrionis, T.D. ; Koutiva, X.I. ; Vovos, N.A.,"A Genetic Algorithm-Based Low Voltage Ride-Through Control Strategy for Grid Connected Doubly Fed Induction Wind Generators", IEEE Transactions on Power Systems, Volume: 29, 2014 ,pp: 1325 – 1334

[10] da Costa, J.P. ; Pinheiro, H. ; Degner, T. ; Arnold, G., "Robust Controller for DFIGs of Grid-Connected Wind Turbines", IEEE Transactions on Industrial Electronics, Volume: 58 , Issue: 9 2011 , pp: 4023 – 4038

[11] Vidal, J. ; Abad, G. ; Arza, J. ; Aurtenechea, S., "Single-Phase DC Crowbar Topologies for Low Voltage Ride Through Fulfillment of High-Power Doubly Fed Induction Generator-Based Wind Turbines", IEEE Transactions on Energy Conversion, Volume: 28 , Issue: 3,2013 , pp: 768 – 781

[12] Abbey, C. ; Joos, G., "Super-capacitor Energy Storage for Wind Energy Applications", IEEE Transactions on Industry Applications, Volume: 43 , Issue: 3 : 2007 , pp: 769 – 776

[13] Guo, W. ; Xiao, L. ; Dai, S. ; Li, Y. ; Xu, X. ; Zhou, W. ; Li, L,"LVRT Capability Enhancement of DFIG With Switch-Type Fault Current Limiter", IEEE Transactions on Industrial Electronics, Volume: 62 , Issue: 1, 2015 , pp: 332 – 342

[14] Wenyong Guo ;Liye Xiao ; Shaotao Dai, "Enhancing Low-Voltage Ride-Through Capability and Smoothing Output Power of DFIG With a Superconducting Fault-Current Limiter–Magnetic Energy Storage System", IEEE Transactions on Energy Conversion, Volume: 27 , Issue: 2, 2012 , pp: 277 – 295.

[15] Li Wang ;Dinh-Nhon Truong, "Stability Enhancement of DFIG-Based Offshore Wind Farm Fed to a Multi-Machine System Using a STATCOM", IEEE Transactions on Power Systems, Volume: 28 , Issue: 3 : 2013 , pp: 2882 – 2889.

[16] Wei Qiao ;Venayagamoorthy, G.K. ; Harley, R.G., "Real-Time Implementation of a STATCOM on a Wind Farm Equipped With Doubly Fed Induction Generators", IEEE Transactions on Industry Applications, Volume: 45 , Issue: 1 : 2009 , pp: 98 – 107.

[17] Li Wang ; Chia-Tien Hsiung, "Dynamic Stability Improvement of an Integrated Grid-Connected Offshore Wind Farm and Marine-Current Farm Using a STATCOM", IEEE Transactions on Power Systems, Volume: 26 , Issue: 2 : 2011 , pp: 690 – 698.

[18] Wei Qiao ; Harley, R.G. ; Venayagamoorthy, G.K., "Coordinated Reactive Power Control of a Large Wind Farm and a STATCOM Using Heuristic Dynamic Programming", IEEE Transactions on Energy Conversion, Volume: 24 , Issue: 2 2009 , pp: 493 – 503

[19] Bozhko, Serhiy ; Asher, G. ; Risheng Li ; Clare, J. ; Liangzhong Yao, "Large Offshore DFIG-Based Wind Farm With Line-Commutated HVDC Connection to the Main Grid: Engineering Studies" IEEE Transactions on Energy Conversion, Volume: 23 , Issue: 1, 2008 , pp: 119 – 127

[20] Bozhko, S.V. ; Blasco-Gimenez, R. ; Risheng Li ; Clare, J.C. ; Asher, G.M., "Control of Offshore DFIG-Based Wind Farm Grid With Line-Commutated HVDC Connection", IEEE Transactions on Energy Conversion, Volume: 22 , Issue: 1, 2007 , pp: 71 – 78

[21] Lingling Fan ; Zhixin Miao,"Mitigating SSR Using DFIG-Based Wind Generation", IEEE Transactions on Sustainable Energy, Volume: 3 , Issue: 3, 2012 , pp: 349 – 358

[22] Ibrahim, A.O. ; ThanhHai Nguyen ; Dong-Choon Lee ; Su-Chang Kim, "A Fault Ride-Through Technique of DFIG Wind Turbine Systems Using Dynamic Voltage Restorers", IEEE Transactions on Energy Conversion, Volume: 26 , Issue: 3, 2011 , pp: 871 – 882

[23] Wessels, C. ; Gebhardt, F. ; Fuchs, F.W., "Fault Ride-Through of a DFIG Wind Turbine Using a Dynamic Voltage Restorer During Symmetrical and Asymmetrical Grid Faults", IEEE Transactions on Power Electronics, Volume: 26 , 2011 , pp: 807 - 815

[24] Alaraifi, S. ; Moawwad, A. ; El Moursi, M.S. ; Khadkikar, V, "Voltage Booster Schemes for Fault Ride-Through Enhancement of Variable Speed Wind Turbines", IEEE Transactions on Sustainable Energy, Volume: 4 , Issue: 4, 2013 , pp: 1071 – 1081

[25] Li Wang ; Hao-Wen Li ; Cheng-Tai Wu,"Stability Analysis of an Integrated Offshore Wind and Seashore Wave Farm Fed to a Power Grid Using a Unified Power Flow Controller", IEEE Transactions on Power Systems, Volume: 28 ,2013 , pp: 2211 – 2221

[26] Karaipoom, T. ;Ngamroo, I.,"Optimal Superconducting Coil Integrated Into DFIG Wind Turbine for Fault Ride Through Capability Enhancement and Output Power Fluctuation Suppression",IEEE Transactions on Sustainable Energy, Volume: 6 , 2015 .

[27] Gayathri, T, Ananth, D.V.N, Kumar, G.V.N, Sivanagaraju G, "Enhancement in Dynamic and LVRT Behavior of an EFOC Controlled DFIG with Integrated Battery Energy Storage System", Proc. IEEE INDICON, 2013 , pp: 1 – 6.

[28] Hua Geng, Cong Liu, Geng Yaung, "LVRT capability of DFIG-Based WECS under Asymmetrical Grid Fault Condition", IEEE Trans. Ind. Elect., Vol.60, o.6, June 2013, pp.2495-2509.

[29] Ananth DVN, NageshKumar GV., "Fault ride-through enhancement using an enhanced field oriented control technique for converters of grid connected DFIG and STATCOM for different types of faults", ISA Transactions (2015), http://dx.doi.org/10.1016/j.isatra.2015.02.014i